Tau pathology mediates the effects of amyloid on neocortical tau propagation and neurodegeneration among non-demented individuals

Murat Bilgel[1*], Dean F. Wong[2], Abhay R. Moghekar[3], Luigi Ferrucci[4], Susan M. Resnick[1], the Alzheimer's Disease Neuroimaging Initiative [†]

[1]Brain Aging and Behavior Section, Laboratory of Behavioral Neuroscience, National Institute on Aging, Baltimore, Maryland, United States; [2]Mallinckrodt Institute of Radiology, Washington University School of Medicine, St. Louis, Missouri, United States; [3]Department of Neurology, Johns Hopkins University School of Medicine, Baltimore, Maryland, United States; [4]Longitudinal Studies Section, Translational Gerontology Branch, National Institute on Aging, Baltimore, Maryland, United States

***For correspondence:** murat.bilgel@nih.gov (MB)

[†]A subset of the data used in preparation of this article was obtained from the Alzheimer's Disease Neuroimaging Initiative (ADNI) database (adni.loni.usc.edu). As such, the investigators within the ADNI contributed to the design and implementation of ADNI and/or provided data but did not participate in analysis or writing of this report. A complete listing of ADNI investigators can be found at: http://adni.loni.usc.edu/wp-content/uploads/how_to_apply/ADNI_Acknowledgement_List.pdf

Abstract Amyloid-β (Aβ) pathology is associated with greater tau pathology and facilitates tau propagation from the medial temporal lobe (MTL) to the neocortex, where tau is closely associated with local neurodegeneration. The degree of the involvement of Aβ versus existing tau pathology in tau propagation and neurodegeneration has not been fully elucidated in human studies. Careful quantification of these effects can inform the development and timing of therapeutic interventions. We conducted causal mediation analyses to investigate these questions in two longitudinal studies of individuals without dementia. As proxies of neurodegeneration, we investigated cerebral blood flow (CBF), glucose metabolism, and regional volume. We first confirmed that Aβ moderates the association between tau in the entorhinal cortex and in the inferior temporal gyrus, a neocortical region exhibiting early tau pathology (amyloid group × entorhinal tau interaction term $\beta = 0.486, \mathrm{SE} = 0.126, p < 0.001$ in the Baltimore Longitudinal Study of Aging [BLSA]; $\beta = 0.658, \mathrm{SE} = 0.137, p < 0.001$ in the Alzheimer's Disease Neuroimaging Initiative [ADNI]). In causal mediation analyses accounting for this facilitating effect of amyloid, amyloid positivity had a statistically significant direct effect on inferior temporal tau as well as an indirect effect via entorhinal tau (average direct effect [ADE]= 0.46, $p < 0.001$ and average causal mediation effect [ACME]= 0.46, $p = 0.0012$ in BLSA; ADE= 0.47, $p < 0.001$ and ACME= 0.254, $p = 0.021$ in ADNI). Entorhinal tau mediated up to 50% of the total effect of amyloid on inferior temporal tau. Higher inferior temporal tau was associated with lower colocalized CBF, glucose metabolism, and regional volume, whereas amyloid had only an indirect effect on these measures via tau, implying tau as the primary driver of neurodegeneration (amyloid–CBF indirect effect ACME $= -0.29$, $p = 0.014$ in BLSA; amyloid–volume indirect effect ACME $= -0.23$, $p < 0.001$ in ADNI). Our findings suggest targeting amyloid or MTL tau might slow down neocortical spread of tau and subsequent neurodegeneration, but a combination therapy may yield better outcomes.

Introduction

In post mortem studies, hyperphosphorylated tau protein aggregates are found universally in the medial temporal lobe (MTL) among individuals over the age of 70 regardless of cognitive status (***Nelson et al., 2012***). Among cognitively unimpaired individuals, the prevalence of temporal lobe tau pathology increases with age (***Jack et al., 2017***). Tau pathology spreads from the MTL to the neocortex primarily via synaptic connections (***Liu et al., 2012***; ***Calafate et al., 2015***; ***De Calignon et al., 2012***; ***Wu et al., 2016***). Amyloid-β (Aβ) can induce tau hyperphosphorylation (***Jin et al., 2011***) and also facilitate trans-synaptic tau transmission (***Pooler et al., 2015***). A longitudinal study of participants who were cognitively normal or had varying degrees of clinical impairment found that levels of Aβ and MTL tau pathology were independently associated with greater rates of change in inferior temporal gyrus (ITG) tau, and that an interaction between rhinal cortex tau and Aβ load accounted for about 35% of the variance in the rate of change in ITG tau (***Sanchez et al., 2021***), providing evidence that Aβ accelerates the propagation of tau. In agreement with this finding, several observational studies found that Aβ was associated with faster tau accumulation over time (***Buckley et al., 2019***; ***Jack et al., 2018***; ***Franzmeier et al., 2020b***; ***Jack et al., 2020***; ***Hanseeuw et al., 2019***).

Once tau pathology spreads to the neocortex, it becomes closely linked with neurodegeneration and cognitive symptoms. The spatial distribution of cortical tau overlaps that of local atrophy (***La Joie et al., 2020***). Tau pathology is also associated locally with other markers of neurodegeneration, including lower cerebral blood flow (CBF) (***Rubinski et al., 2021***; ***Albrecht et al., 2020***), glucose metabolism (***Strom et al., 2021***; ***Hanseeuw et al., 2017***), and volume (***Iaccarino et al., 2018***). However, the extent of neurodegeneration is greater than what is accounted for by tau pathology (***Gómez-Isla et al., 1997***), suggesting that additional factors are involved. One such factor is thought to be Aβ pathology. Studies have found associations between Aβ and greater atrophy (***Chételat et al., 2010***) and lower hippocampal volumes (***Petersen et al., 2016***; ***Villemagne et al., 2013***) among cognitively normal individuals, lower glucose metabolism among non-demented (***Carbonell et al., 2020***; ***Teipel and Grothe, 2016***) and cognitively normal individuals (***Petersen et al., 2016***), and lower CBF in a sample consisting mostly of individuals without dementia (***Rubinski et al., 2021***). Additionally, one study found an interaction between Aβ and tau in relation to glucose metabolism among patients with clinically diagnosed Alzheimer's disease (AD) (***Bischof et al., 2016***).

Prior literature provides strong evidence for the involvement of both Aβ pathology and MTL tau in propagating tau to the neocortex. However, the extent to which Aβ versus existing MTL tau pathology is involved in propagating tau among individuals without dementia remains unclear. An important consideration in the investigation of this question is the facilitating effect of Aβ on tau spread, which requires modeling the interaction between Aβ and MTL tau in relation to neocortical tau using mediation analysis to accurately quantify their relative contributions. Similarly, while previous research has highlighted tau, rather than Aβ, as the driver of neurodegeneration (***Mak et al., 2018***; ***Scott et al., 2020***) and speculated that tau may mediate the effects of Aβ on cortical neurodegeneration (***Gordon et al., 2018***), these studies have not formally assessed this using mediation analysis.

It is important to quantify the degree of involvement of Aβ and tau pathologies in the propagation of tau and neurodegeneration, as these findings may inform the development and timing of therapeutic interventions to prevent or delay the onset of clinical symptoms. If the propagation of tau and neurodegeneration are mainly driven by existing tau pathology, then interventions to alleviate Aβ pathology would not be expected to prevent the cortical spreading of tau or neurodegenerative changes. On the other hand, if Aβ also has a substantial direct effect in the neocortical propagation of tau or neurodegeneration, then successful therapies among individuals who already have some level of MTL tau would need to target both neuropathologies simultaneously.

In this study, we first verify that Aβ facilitates the spread of tau from MTL to the neocortex, and then focus on two scientific questions: (1) To what extent is neocortical tau accumulation driven

by Aβ versus MTL tau pathology? (2) To what extent is neuronal activity, metabolism, or regional volume loss driven by Aβ versus local tau pathology? We examine these two questions among individuals without dementia in two distinct longitudinal studies, the Baltimore Longitudinal Study of Aging (BLSA) and the Alzheimer's Disease Neuroimaging Initiative (ADNI), to gain insight into changes that occur early in the disease process. To verify that Aβ facilitates the spread of tau from the MTL to the neocortex, we investigate whether Aβ moderates the association between tau in the entorhinal cortex (EC) and the ITG. We focus specifically on the ITG for evaluating neocortical tau because it is an early neocortical region exhibiting tau pathology (***Berron et al., 2021***) and has often been used to measure tau pathology among individuals without dementia. To quantify the involvement of Aβ versus MTL tau in propagating tau, we evaluate whether EC tau mediates the association between Aβ and ITG tau using causal mediation analysis. We investigate the local relationships between Aβ and proxies of neurodegeneration in the ITG, including CBF, glucose metabolism, and regional volume, and whether these relationships are mediated by ITG tau. Finally, we use longitudinal data to to assess the directional assumptions of our causal models. Our study substantially builds upon prior work by evaluating certain modeling assumptions with the goal of moving beyond examining associations to enable a causal interpretation of our findings.

Results

Participants

We conducted our analyses separately in the BLSA and ADNI (adni.loni.usc.edu)[1]. These two data sets allowed us to assess our scientific questions in two complementary stages of AD prior to the onset of dementia: most of the BLSA participants were cognitively normal, whereas most of the ADNI participants included in these analyses had MCI. The study samples included participants without dementia who had apolipoprotein E (*APOE*) genotyping, at least one ^{18}F-flortaucipir (FTP) PET scan, as well as a T_1-weighted MRI and an amyloid PET scan within 3.5 years of their baseline FTP PET scan. The radiotracer used for amyloid PET was ^{11}C-Pittsburgh compound B (PiB) in the BLSA and ^{18}F-florbetapir (FBP) in the ADNI. Amyloid status was determined using established mean cortical thresholds of 1.06 distribution volume ratio (DVR) in the BLSA (***Bilgel et al., 2019***) and 1.11 standardized uptake value ratio (SUVR) in the ADNI (***Schreiber et al., 2015***). Dynamic amyloid PET acquisition in the BLSA allowed for the computation of the relative radiotracer delivery parameter R_1, which is a surrogate measure of CBF (***Bilgel et al., 2019***). In the ADNI, instead of CBF, we used a measure of glucose metabolism as assessed by ^{18}F-fluorodeoxyglucose (FDG) PET[2]. Both CBF and glucose metabolism are correlates of neuronal activity (***Sokoloff, 1993***). ADNI participants without an FDG PET scan within 3.5 years of their baseline FTP PET or of the corresponding amyloid PET scans were excluded from the study sample. Each PET and MRI measure was converted to a z-score for the statistical analyses, but their original values were used for the summary table and scatter plots.

Participant characteristics are presented in ***Table 1***. 103 BLSA and 122 ADNI participants were included in the analyses. The percentage of participants who were amyloid positive (A+) was 31% in the BLSA and 50% in the ADNI, which are comparable to the percentages reported in other samples of cognitively normal older individuals and individuals with MCI, respectively (***Jansen et al., 2015***). Regional FTP PET SUVRs were higher in the ADNI, but these values are not directly comparable between the studies due to differences in image processing.

[1]The ADNI was launched in 2003 as a public-private partnership, led by Principal Investigator Michael W. Weiner, MD. The primary goal of ADNI has been to test whether serial magnetic resonance imaging (MRI), positron emission tomography (PET), other biological markers, and clinical and neuropsychological assessment can be combined to measure the progression of mild cognitive impairment (MCI) and early AD.

[2]While the ADNI study includes arterial spin labeling (ASL)-MRI to quantify CBF, our inclusion criteria resulted in a very small sample for the ASL-MRI measures. Because of this, we chose to use FDG PET measures instead.

Causal mediation analyses

(1) To what extent is neocortical tau accumulation driven by Aβ versus MTL tau pathology? We first verified that Aβ facilitates the spread of tau from the MTL to the neocortex. To do this, we visually confirmed that the association between EC and ITG tau differs by amyloid status (***Figure 1***) and assessed if there is an interaction between amyloid status and MTL tau in relation to ITG tau using a linear regression model adjusted for age at FTP PET, sex, *APOE* $\varepsilon 4$ positivity, and years of education. As expected, both amyloid positivity and higher EC tau was associated with higher ITG tau and the A+ group exhibited a stronger correlation between the levels of tau pathology in these two regions (amyloid $\times$ EC tau interaction term $\beta = 0.486, \mathrm{SE} = 0.126, p < 0.001$ in the BLSA; $\beta = 0.658, \mathrm{SE} = 0.137, p < 0.001$ in the ADNI).

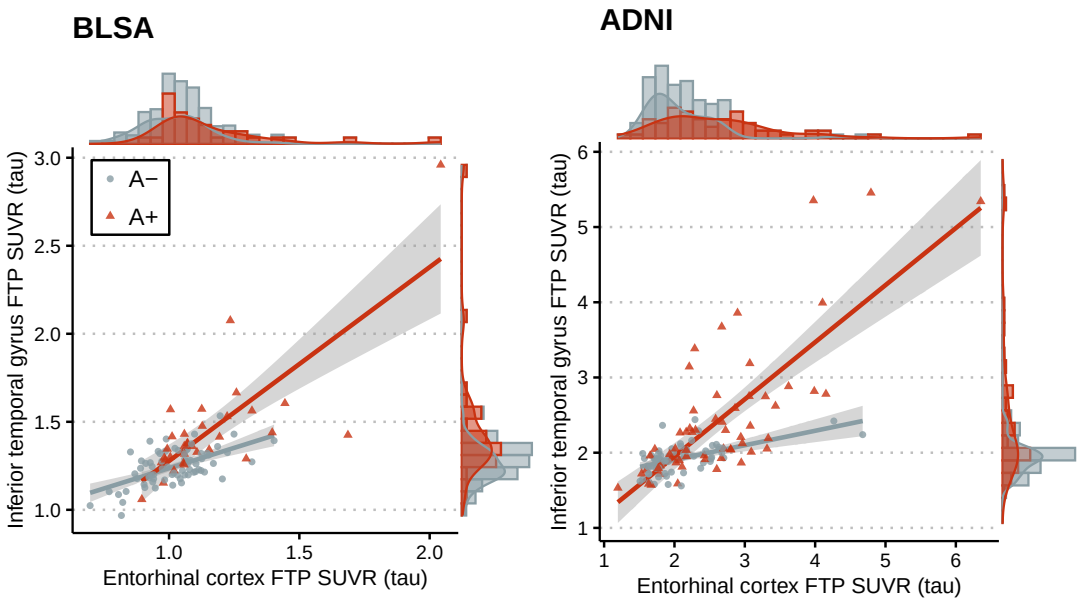

Figure 1. Scatter plots of inferior temporal gyrus vs. entorhinal cortex tau in the BLSA and ADNI. Higher entorhinal tau was associated with higher inferior temporal gyrus tau in both amyloid– (A-) and A+ groups, with the A+ group exhibiting a stronger positive correlation. ADNI = Alzheimer's Disease Neuroimaging Initiative, BLSA = Baltimore Longitudinal Study of Aging, FTP = flortaucipir, SUVR = standardized uptake value ratio.

We then conducted a causal mediation analysis to examine the extent to which neocortical tau accumulation is driven by Aβ versus MTL tau pathology. The model for the outcome included an interaction between the exposure (amyloid) and the mediator (EC tau). Because of this, the causal mediation analysis involved the estimation of two mediation effects and two direct effects (one per amyloid group). These effects are defined and interpreted within the counterfactual framework (***Pearl, 2014***). The average causal mediation effect (ACME) (also known as the natural indirect effect) for the amyloid negative (A–) group, denoted $\mathrm{ACME}_{\mathrm{A-}}$, is the expected difference in the outcome while amyloid status is fixed at A– and the mediator (tau) changes from the value attained or that would have been attained under amyloid negativity to the value under amyloid positivity for each individual. $\mathrm{ACME}_{\mathrm{A+}}$ is defined similarly, while fixing amyloid status at A+ and changing the mediator from the value attained or would have been attained under A– to the value under A+ for each individual. The average direct effect (ADE) (also known as the natural direct effect) for the A– group, denoted $\mathrm{ADE}_{\mathrm{A-}}$, is the expected difference in the outcome as a result of changing amyloid status from A– to A+ while keeping the mediator at the value observed or that would have been observed under A– for each individual. $\mathrm{ADE}_{\mathrm{A+}}$ is defined similarly, while keeping the mediator at the value observed or that would have been observed under A+ for each individual. For an A– individual, the value of the mediator had they been A+ is a counterfactual (and vice versa), since it

involves imaging a scenario where the mediator is measured under an alternative amyloid status for that individual. ACME and ADE reflect the effect of amyloid on the outcome solely through tau (in the absence of the outcome's ability to respond to a change in amyloid status) and not through tau (in the absence of tau's ability to respond to a change in amyloid status), respectively.

In causal mediation analysis, it is necessary to adjust for covariates that may be confounders of the relationships among the exposure, mediator, and outcome (***Pearl, 2014***). Since *APOE* $\varepsilon 4$ positivity has been shown to impact both Aβ and MTL tau pathology (***Salvadó et al., 2021***; ***Sanchez et al., 2021***), it is necessary to include it as a covariate in our analyses. We also included age at FTP PET, sex, and years of education as covariates.

We found that the effect of amyloid on ITG tau was mediated by EC tau ($\text{ACME}_{\text{A}-} = 0.28$, $p = 0.0012$ and $\text{ACME}_{\text{A}+} = 0.634$, $p = 0.0012$ in the BLSA; $\text{ACME}_{\text{A}-} = 0.108$, $p = 0.021$ and $\text{ACME}_{\text{A}+} = 0.4$, $p = 0.021$ in the ADNI) (***Figure 2***). In addition to this mediation effect, amyloid had a direct effect on ITG tau ($\text{ADE}_{\text{A}-} = 0.28$, $p = 0.05$ and $\text{ADE}_{\text{A}+} = 0.635$, $p < 0.001$ in the BLSA; $\text{ADE}_{\text{A}-} = 0.328$, $p = 0.073$ and $\text{ADE}_{\text{A}+} = 0.619$, $p < 0.001$ in the ADNI) (***Figure 2***).

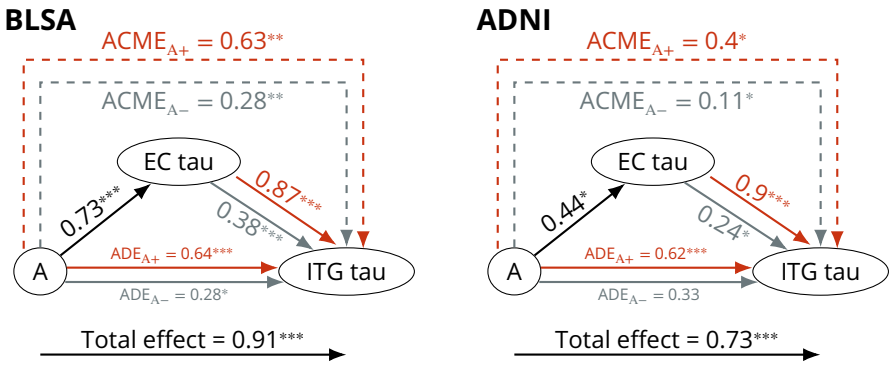

Figure 2. Causal mediation analysis results for the model investigating the relationships among amyloid group (A) and tau in the entorhinal cortex (EC) and the inferior temporal gyrus (ITG) in the BLSA (*left*) and the ADNI (*right*). The effect of amyloid on ITG tau is mediated by EC tau. Arrow from A to EC tau indicates the linear regression coefficient, and the gray and red arrows from EC tau to ITG tau indicate the linear regression coefficients for the amyloid negative and positive groups, respectively. Both the mediator and the outcome models were adjusted for age, sex, *APOE* $\varepsilon 4$ positivity, and years of education. ACME = average causal mediation effect, ADE = average direct effect. *** $p < .001$, ** $p < .01$, * $p < .05$.

Figure 2–Figure supplement 1. Sensitivity analyses.

Finally, we assessed the sensitivity of our mediation analysis results to the sequential ignorability assumption that there are no unspecified confounders between the mediator and the outcome using a parametric sensitivity analysis based on the residual correlation between the mediator and the outcome (***Imai et al., 2010***). In both datasets, $\text{ACME}_{\text{A}+}$ was robust to violations of the assumption that there are no unspecified confounders between the mediator (EC tau) and the outcome (ITG tau) (***Figure 2–Figure Supplement 1***).

(2) To what extent is neuronal activity, metabolism, or regional volume loss driven by Aβ versus local tau pathology?

We conducted a separate causal mediation analysis to investigate the direct and indirect effects of Aβ on proxies of ITG neurodegeneration. As in the causal mediation analysis for our first research question, we included age, sex, *APOE* $\varepsilon 4$ positivity, and years of education as covariates. However, the inclusion of an interaction between the exposure (amyloid) and mediator (ITG tau) did not yield a statistically significant improvement in the residual sum of squares for any of the models investigating proxies of ITG neurodegeneration as outcomes, and therefore, this interaction was not included in the final models.

The effect of amyloid positivity on ITG CBF was mediated via ITG tau in the BLSA (ACME $= -0.292$, $p = 0.014$) (***Figure 3***), and the effect of amyloid positivity on ITG volume was mediated via ITG tau in

the ADNI (ACME $= -0.234$, $p < 0.001$) (***Figure 4***). Additionally, there was a trend-level direct effect of amyloid positivity on ITG CBF (ADE $= -0.44$, $p = 0.054$).

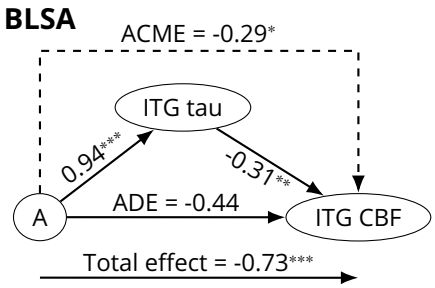

Figure 3. Causal mediation analysis results for the model investigating the relationships among amyloid group (A), tau in the ITG, and CBF in the ITG in the BLSA. The effect of amyloid on ITG CBF was mediated via ITG tau. Arrows from A to ITG tau and from ITG tau to ITG CBF indicate the linear regression coefficients for these associations. Both the mediator and the outcome models were adjusted for age, sex, *APOE* $\varepsilon 4$ positivity, and years of education. ACME = average causal mediation effect, ADE = average direct effect. *** $p < .001$, ** $p < .01$, * $p < .05$.

Figure 3–Figure supplement 1. Sensitivity analysis.

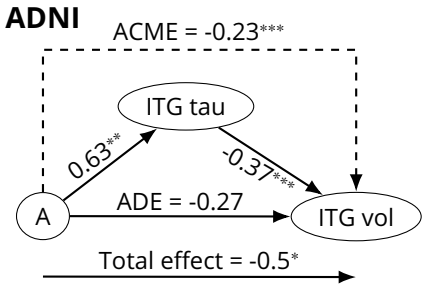

Figure 4. Causal mediation analysis results for the model investigating the relationships among amyloid group (A), tau in the ITG, and ITG volume in the ADNI. The effect of amyloid on ITG volume was mediated via ITG tau. Arrows from A to ITG tau and from ITG tau to ITG volume indicate the linear regression coefficients for these associations. Both the mediator and the outcome models were adjusted for age, sex, *APOE* $\varepsilon 4$ positivity, and years of education. ACME = average causal mediation effect, ADE = average direct effect. *** $p < .001$, ** $p < .01$, * $p < .05$.

Figure 4–Figure supplement 1. Sensitivity analysis.

Sensitivity analysis demonstrated that these ACME estimates are not as robust as our other findings to violations of the assumption of no unspecified confounders between the mediator (ITG tau) and the outcome (ITG CBF or volume) (***Figure 3–Figure Supplement 1*** and ***Figure 4–Figure Supplement 1***, respectively).

We do not report the results of the mediation analysis investigating ITG volume in the BLSA or ITG glucose metabolism in the ADNI since the associations between amyloid and these variables were small and not statistically significant (total effect on ITG volume in the BLSA $= -0.26$, $p = 0.26$; total effect on ITG glucose metabolism in the ADNI $= -0.026$, $p = 0.88$).

Further examination of causal assumptions

In addition to the causal mediation sensitivity analyses described above, we conducted two analyses to further examine the assumptions of our causal modeling. The first of these analyses, based on evaluating conditional independencies between variables, was aimed to assess whether our overarching causal model is inconsistent with the data and if a model with sparser connections between variables is possible. The second analysis was aimed to assess whether longitudinal data provide support for the assumed causal directions among amyloid, tau, and neurodegeneration.

Conditional independencies

The overarching directed acyclic graph (DAG) motivating our causal mediation analyses is presented in ***Figure 5***. While there is no statistical approach for proving this graph using observational data, falsification tests can be conducted to determine if the graph is inconsistent with the data by assessing conditional independencies implied by this DAG. The only implied conditional independence by this DAG is that EC tau and ITG neurodegeneration (i.e., CBF in the BLSA, glucose metabolism in the ADNI, and regional volume) are independent given amyloid, ITG tau, and the covariates (age, sex, *APOE* $\varepsilon 4$ positivity, and education). We examined this conditional independency for each neurodegeneration measure using partial correlation. The partial correlation between EC tau and ITG CBF given amyloid status and all covariates was small and not statistically significant in the BLSA ($\rho = 0.116$, $p = 0.26$). Similarly, the partial correlation between EC tau and ITG glucose metabolism was small and not statistically significant in the ADNI ($\rho = -0.169$, $p = 0.07$). The partial correlation between EC tau and ITG volume given amyloid status and all covariates was also small and not statistically significant in both the BLSA ($\rho = 0.162$, $p = 0.11$) and the ADNI ($\rho = -0.166$, $p = 0.075$). These results are in agreement with the conditional independency implied by our DAG. We also assessed more parsimonious versions of this model (i.e., DAGs with fewer edges) by testing their implied conditional independencies using partial correlations, but none satisfied all implied conditional dependencies (***Appendix 1***). Of note, even though the indirect effect of amyloid on neurodegeneration was not statistically significant in the causal mediation analyses, removing the arrow from amyloid to neurodegeneration in the DAG yielded a conditional independence (i.e., that amyloid and ITG neurodegeneration are independent given ITG tau and the covariates) that was not consistent with the data.

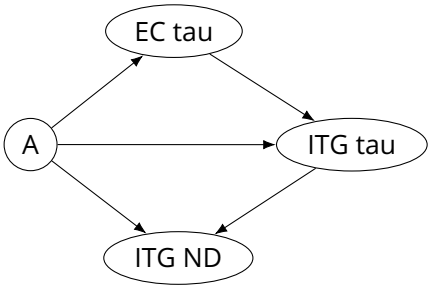

Figure 5. DAG representing the causal model for amyloid (A), tau, and neurodegeneration (ND). As neurodegeneration measures, we investigated CBF (in the BLSA only), glucose metabolism (in the ADNI only), and regional volume. Common covariates for all four nodes are not shown in this figure. These covariates include age, sex, *APOE* $\varepsilon 4$ positivity, and education.

Longitudinal analyses

We expected to find evidence using longitudinal data in support of the directions assumed among the variables in our DAG. For example, based on our model assumption that amyloid causally contributes to ITG tau, we expected to find an association between amyloid positivity and the longitudinal rate of tau accumulation in the ITG. We examined such associations in our data using linear mixed effects models.

In the BLSA, we did not find a statistically significant association between the rate of change in EC tau and amyloid status ($\beta = 0.0789, \mathrm{SE} = 0.0605, p = 0.198$), or between the rate of change in ITG tau and amyloid status ($\beta = 0.0427, \mathrm{SE} = 0.0391, p = 0.28$) or baseline EC tau ($\beta = -0.0297, \mathrm{SE} = 0.0273, p = 0.281$). In the ADNI, A+ individuals had steeper increases in EC tau over time ($\beta = 0.0675, \mathrm{SE} = 0.0328, p = 0.043$), and there was a trend-level association with amyloid positivity and rate of change in ITG tau ($\beta = 0.0536, \mathrm{SE} = 0.0299, p = 0.077$). Higher baseline EC tau was associated with a steeper increase in the ITG tau over time ($\beta = 0.0799, \mathrm{SE} = 0.0199, p < 0.001$).

We also investigated whether ITG tau is associated with the rate of change in ITG CBF, glucose

metabolism, or volume. The outcome variable was ITG CBF (in the BLSA), glucose metabolism (in the ADNI), or volume. We did not find an association between amyloid status and the rate of change in ITG CBF ($\beta = 0.0145, \mathrm{SE} = 0.0313, p = 0.644$ in the BLSA), glucose metabolism ($\beta = -0.00672, \mathrm{SE} = 0.0399, p = 0.867$ in the ADNI), or volume ($\beta = -0.0129, \mathrm{SE} = 0.0228, p = 0.573$ in the BLSA; $\beta = -0.00217, \mathrm{SE} = 0.0407, p = 0.958$ in the ADNI). Higher baseline ITG tau was associated with a steeper decrease in ITG glucose metabolism ($\beta = -0.0901, \mathrm{SE} = 0.0396, p = 0.026$) and ITG volume over time ($\beta = -0.0487, \mathrm{SE} = 0.0139, p < 0.001$ in the BLSA; $\beta = -0.0644, \mathrm{SE} = 0.0237, p = 0.008$ in the ADNI), but not with the rate of change in ITG CBF ($\beta = 0.029, \mathrm{SE} = 0.019, p = 0.13$).

Discussion

In both the BLSA and the ADNI, greater EC tau was associated with greater ITG tau and this association was stronger among amyloid positive individuals. These findings agree with prior reports that Aβ facilitates the spread of tau from the MTL to the neocortex.

Amyloid's association with ITG tau was in part mediated by EC tau: EC tau mediated 50% of the total effect in the BLSA and 35% in the ADNI. This mediation effect was robust to the sequential ignorability assumption of causal mediation analysis, meaning that any unspecified confounder of the mediator and outcome relationship must have substantially correlated effects on these two variables in order for our reported mediation effects to become statistically non-significant.

Higher ITG tau was associated with several proxies of neurodegeneration in the same region, including CBF, glucose metabolism, and volume (in ADNI only). While we did not find a direct effect of amyloid positivity on neurodegeneration, it had an indirect effect via tau pathology on CBF (BLSA) and volume (ADNI). The indirect effect of amyloid via ITG tau accounted for 40% of the total effect on ITG CBF in the BLSA and 47% of the total effect on ITG volume in the ADNI, but the statistical significance of these indirect effect estimates was sensitive to the assumption that there were no unspecified confounders of ITG tau and neurodegeneration.

In longitudinal analyses, amyloid positivity was associated with steeper increases in EC tau, and that greater EC tau at baseline was associated with steeper increases in ITG tau in the ADNI. The lack of statistically significant amyloid associations in the BLSA might be due to insufficient statistical power to detect small longitudinal effects among cognitively normal individuals (***Harrison et al., 2018***). Greater ITG tau at baseline was associated with steeper decreases in glucose metabolism in the same region. The finding that greater ITG tau at baseline is associated with faster volume loss was shared between the BLSA and the ADNI.

Our findings may have therapeutic implications. The causal mediation results suggest that treating EC tau alone would likely be insufficient in preventing the neocortical spread of tau, since the direct path between amyloid and ITG tau would not be affected. Similarly, preventing amyloid alone among individuals who already have some level of EC tau would also likely be insufficient, since EC tau would continue to spread to the neocortex. However, given the synergistic association between amyloid and EC tau in neocortical propagation, targeting either pathology would be expected to slow down the spread of tau to the neocortex. A recent clinical trial of donanemab, an anti-amyloid monoclonal antibody, conducted among patients with early symptomatic AD failed to find a difference in global tau load between treatment and placebo groups, but there was a greater reduction in tau accumulation in frontal and temporal regions (***Mintun et al., 2021***). An amyloid intervention earlier in the disease course, combined with a tau-targeting therapy, might yield more pronounced effects on neocortical tau.

Tau, rather than amyloid, might be the main driver of neurodegeneration. In the recently completed phase 2 trial among patients with mild AD of AADvac1, an active immunotherapy against pathological tau, neurodegeneration was slower in the treatment group, as evidenced by an attenuated increase in neurofilament light (***Novak et al., 2021***). This clinical trial result supports our model assumption that tau is a contributor but also aligns with previous reports that tau pathology does not explain the entire degree of neurodegeneration (***Gómez-Isla et al., 1997***). We did

not observe an interaction between amyloid and neocortical tau in relation to neurodegeneration, while such a synergistic relationship has been reported in transgenic mice (***Pooler et al., 2015***) and human (***Hanseeuw et al., 2017***) studies.

Our finding that tau pathology was associated with volume in the ADNI but not in the BLSA might be explained by differences in the composition of the samples: most ADNI participants included in our analyses had MCI, whereas most BLSA participants were cognitively normal. This difference between the two samples suggests that the detrimental effects of tau pathology on volume loss might not be evident until later stages of disease. Supporting this hypothesis, a simulation study based on quantitative neuron loss and neurofibrillary tangle (NFT) formation data suggested that neurons harboring NFTs may survive for about two decades (***Morsch et al., 1999***). Our findings in the BLSA might reflect differences in the temporal sequence of changes. CBF might exhibit neuropathology-associated changes while individuals are cognitively normal, prior to declines in regional brain volumes (***Sperling et al., 2011***). This could explain the absence of a cross-sectional association of tau with volume in the BLSA and the presence of an association with CBF.

Our longitudinal findings in the ADNI provide support for most of the causal directions assumed in our DAG (***Figure 5***), with one notable exception being the path from amyloid to neurodegeneration. In analyses adjusted for tau, we did not find an association between amyloid positivity and rate of change in any of the neurodegeneration measures we assessed. The lack of an association suggests that the direct effect of fibrillar amyloid on neurodegenerative change is small and requires larger samples to be detected, or that fibrillar amyloid is not a direct player in CBF, glucose metabolism, or volume loss changes among individuals without dementia.

Limitations of our study include the small samples and the lack of measures for other factors implicated in tau spread (i.e., neuroinflammation or synaptic markers), which prevents the analysis of competing mechanisms. Functional (***Franzmeier et al., 2020a***) and structural (***Jacobs et al., 2018***) connections between regions have been shown to be associated with the propagation of tau and could be important mediators of the association between amyloid and neocortical tau. We used binary amyloid status based on fibrillar Aβ burden, but a measure of soluble Aβ could have been more appropriate given the evidence that soluble forms induce tau hyperphosphorylation (***Jin et al., 2011***) and may be more closely involved in neurodegeneration rather than fibrillar amyloid. However, concentrations of soluble Aβ oligomers correlate with the amount of Aβ plaques, albeit weakly, among individuals without dementia (***Esparza et al., 2013***). It is also possible that there are mechanisms by which cortical fibrillar amyloid deposition can influence MTL tau pathology; for example, amyloid pathology is associated with axonal dystrophy (***McKee et al., 1991***), which might be a mechanism by which neocortical amyloid exerts retrograde effects. While we assumed a unidirectional association between amyloid and tau, it is possible that these pathologies exist within a feedback loop. One study suggested that amyloid and tau pathology reinforce each other (***Pooler et al., 2015***). There are differing schools of thought about the sequence of changes in CBF and tau (***Korte et al., 2020***). It is unclear whether PET measures of CBF would reliably detect the types of early changes that are hypothesized to lead to tau pathology. Extensive longitudinal data will be necessary to determine the direction of these associations. The measures we used to assess neurodegeneration are not direct measures of neurodegeneration but rather proxies. Of note, cerebral amyloid angiopathy, which can be detected using amyloid PET but with low specificity, has direct effects on cerebrovascular function. This confound might impact the interpretation of cerebral blood flow as an indicator of neuronal activity.

An important strength of our study is the replication of many of our findings in two longitudinal cohorts. In particular, the causal mediation analysis findings regarding amyloid-facilitated propagation of tau from the MTL to the neocortex were highly consistent in the BLSA and the ADNI despite differences in sample composition. Based on this consistency, we expect these findings to be generalizable to similar samples of individuals without dementia.

In conclusion, our study confirms the facilitating role of amyloid in the propagation of tau from the MTL to the neocortex among cognitively normal individuals and in MCI. Since entorhinal tau

mediated only up to half of the association of amyloid with neocortical tau, we speculate that interventions to reduce only entorhinal tau or only amyloid among individuals who already have MTL tau might slow but not fully prevent the neocortical spread of tau. Preventing neocortical tau early in the course of neuropathology might be an important element in preventing cortical neurodegeneration, including lower CBF, hypometabolism, and volume loss. It will be important to examine the potential impact of reducing amyloid and tau on cognitive decline in future studies and to determine if preventing the spread of tau from the MTL to the neocortex would yield clinical benefit.

Materials and Methods

In the BLSA, cognitively normal (CN) status was based on either (i) a Clinical Dementia Rating (CDR) (***Morris, 1993***) of zero and ≤ 3 errors on the Blessed Information-Memory-Concentration Test (***Fuld, 1978***), and therefore the participant did not meet criteria for consensus conference; or (ii) the participant met criteria for consensus conference and was determined to be CN based on thorough review of clinical and neuropsychological data. MCI diagnoses were determined according to Petersen criteria (***Petersen, 2004***). At enrollment into the PET neuroimaging substudy of the BLSA, all participants were free of central nervous system (CNS) disease (dementia, stroke, bipolar illness, epilepsy), severe cardiac disease, severe pulmonary disease, and metastatic cancer. The assessment of cognitive status and enrollment criteria in the ADNI are described elsewhere (***Petersen et al., 2010***).

The BLSA research protocols were conducted in accordance with United States federal policy for the protection of human research subjects contained in Title 45 Part 46 of the Code of Federal Regulations (45 CFR 46), approved by local institutional review boards (IRB), and all participants gave written informed consent at each visit. The BLSA PET substudy is governed by the IRB of the Johns Hopkins Medical Institutions, and the BLSA study is overseen by the National Institute of Environmental Health Sciences IRB. The ADNI study was approved by the IRBs of all of the participating institutions and all participants gave written informed consent.

MR imaging

BLSA

Magnetization-prepared rapid gradient echo (MPRAGE) scans were acquired on a 3 T Philips Achieva scanner (repetition time (TR) = $6.8\,\mathrm{ms}$, echo time (TE) = $3.2\,\mathrm{ms}$, flip angle = 8°, image matrix = 256×256, 170 slices, voxel size = $1\,\mathrm{mm} \times 1\,\mathrm{mm} \times 1.2\,\mathrm{mm}$). We computed anatomical labels and regional brain volumes using Multi-atlas region Segmentation using Ensembles of registration algorithms and parameters (MUSE) (***Doshi et al., 2016***) and intracranial volume (ICV) was determined from intracranial masks computed using a deep learning approach (***Doshi et al., 2019***). We computed ICV-adjusted residuals for ITG volume using the approach described by ***Jack et al.*** (***1989***).

ADNI

For a detailed description of MRI protocols, see adni.loni.usc.edu. We used tabular data provided by the ADNI MRI Core at the University of California San Francisco for regional volumes. These were obtained with cross-sectional FreeSurfer 6.0 (https://surfer.nmr.mgh.harvard.edu/) processing of MPRAGE/IRSPGR scans based on the Desikan-Killiany atlas (***Desikan et al., 2006***). We computed ICV-adjusted residuals for ITG volume as described for the BLSA.

PET imaging

BLSA

FTP PET scans were obtained over $30\,\mathrm{min}$ on a Siemens High Resolution Research Tomograph (HRRT) scanner starting $75\,\mathrm{min}$ after an intravenous bolus injection of approximately $370\,\mathrm{MBq}$ of radiotracer. Dynamic images were reconstructed using ordered subset expectation-maximization to yield 6 time frames of $5\,\mathrm{min}$ each with approximately $2.5\,\mathrm{mm}$ full-width at half-maximum (FWHM) at

the center of the field of view (image matrix = 256×256, 207 slices, voxel size = $1.22\,\mathrm{mm} \times 1.22\,\mathrm{mm} \times 1.22\,\mathrm{mm}$). Following time frame alignment, the $80\,\mathrm{min}$ to $100\,\mathrm{min}$ average PET image was partial volume corrected using the region-based voxelwise method (***Thomas et al., 2011***). The corrected image was then used to compute SUVR images using the inferior cerebellar gray matter as the reference region. FTP PET image analysis workflow is described in more detail in ***Ziontz et al.*** (***2019***). We computed the average bilateral SUVR in the EC and the ITG.

PiB PET scans were obtained over $70\,\mathrm{min}$ on either a GE Advance or a Siemens HRRT scanner immediately following an intravenous bolus injection of approximately $555\,\mathrm{MBq}$ of radiotracer. Scans acquired on the GE Advance were reconstructed using filtered backprojection with a ramp filter to yield 33 time frames with approximately $4.5\,\mathrm{mm}$ FWHM at the center of the field of view (image matrix = 128×128, 35 slices, voxel size = $2\,\mathrm{mm} \times 2\,\mathrm{mm} \times 4.25\,\mathrm{mm}$). Scans acquired on the Siemens HRRT were reconstructed using ordered subset expectation-maximization to yield 33 time frames with approximately $2.5\,\mathrm{mm}$ FWHM at the center of the field of view (image matrix = 256×256, 207 slices, voxel size = $1.22\,\mathrm{mm} \times 1.22\,\mathrm{mm} \times 1.22\,\mathrm{mm}$). Since most of the PiB PET scans were acquired on the GE Advance, the reconstructed HRRT scans were smoothed with a $3\,\mathrm{mm}$ FWHM isotropic Gaussian kernel to bring their spatial resolution closer to that of the GE Advance scans, and then resampled to match the voxel size of the GE Advance PiB PET scans. Following time frame alignment and co-registration with MRI, DVR and relative radiotracer delivery (R_1) images were computed using a spatially constrained simplified reference tissue model with cerebellar gray matter as the reference region (***Zhou et al., 2007***). Mean cortical amyloid burden was calculated as the average of the DVR values in cingulate, frontal, parietal (including precuneus), lateral temporal, and lateral occipital cortical regions, excluding the sensorimotor strip. Leveraging longitudinal PiB PET data available on both GE Advance and HRRT scanners for 79 BLSA participants, we estimated the parameters of a linear model mapping mean cortical DVR values between the GE Advance and HRRT scanners, and applied this mapping to all HRRT values to harmonize them with the GE Advance values. Individuals were categorized as amyloid –/+ based on a mean cortical DVR threshold of 1.06, which was derived from a Gaussian mixture model fitted to harmonized mean cortical DVR values at baseline. PiB PET image analysis workflow is described in further detail in ***Bilgel et al.*** (***2019***).

ADNI

For a detailed description of PET protocols, see adni.loni.usc.edu. We used tabulated values provided by the ADNI PET Core at the University of California Berkeley, where image quality control and preprocessing were performed. Here, we provide a brief description of image acquisition and of the processing performed by the ADNI PET Core. FTP PET scans were acquired over $30\,\mathrm{min}$ starting $75\,\mathrm{min}$ after an intravenous bolus injection of approximately $370\,\mathrm{MBq}$ of radiotracer. Images were reconstructed to yield 6 time frames of $5\,\mathrm{min}$ each. FTP values were partial volume corrected using the geometric transfer matrix method (***Rousset et al., 1998***), and inferior cerebellar gray matter was used as the reference region to compute SUVRs. We computed a bilateral entorhinal cortex and a bilateral ITG volume-weighted average FTP SUVR using the tabular data provided in the ADNI database.

FBP PET scans were acquired over $20\,\mathrm{min}$ and reconstructed to yield 4 time frames of $5\,\mathrm{min}$ each. FBP scans started $50\,\mathrm{min}$ after an intravenous bolus injection of approximately $370\,\mathrm{MBq}$ of radiotracer. Whole cerebellum was used as the reference region to compute SUVR images. A global cortical amyloid index was calculated as the mean of frontal, lateral temporal, lateral parietal, and cingulate gray matter regions, and amyloid status was defined using an established cutoff of 1.11 (***Schreiber et al., 2015***).

FDG PET scans were acquired over $30\,\mathrm{min}$ starting $30\,\mathrm{min}$ after an intravenous bolus injection. For FDG, we averaged the left and right temporal lobe components of the meta-region of interest (ROI) reported by ***Landau et al.*** (***2011***), which falls largely within the ITG (but also includes part of the middle temporal gyrus).

Statistical analyses

We converted each continuous PET measure to z-scores using the mean and standard deviation at the visit corresponding to (or closest to) the baseline FTP PET scan for each participant. z-scores were computed separately for the BLSA and the ADNI using data for all participants. In the rest of the Methods section and in the Results, we refer to EC (or ITG) FTP SUVR z-score as EC (or ITG) tau, ITG PiB R_1 z-score as ITG CBF, ITG FDG SUVR z-score as ITG glucose metabolism, and ITG ICV-adjusted volume z-score as ITG volume.

Including race as an additional covariate in the BLSA did not affect the statistical significance of any of our findings. We did not investigate race as a covariate in the ADNI sample given its limited minority representation.

For all analyses, statistical significance was defined as two-tailed $p < 0.05$. Focusing on a single region (ITG) as the indicator of early neocortical tau pathology allowed us to avoid multiple testing. We did not perform multiple comparison correction since we performed one statistical test per family of hypotheses per data set.

Causal mediation analyses

The causal mediation analyses involved two linear regression models: one for the mediator and another for the outcome. All linear regression models included the exposure (i.e., amyloid) as an independent variable. The models for the outcome additionally included the mediator as an independent variable, and the models with ITG tau as the outcome variable also included an interaction between amyloid and EC tau as an explanatory variable. We included age, sex, *APOE* $\varepsilon 4$ positivity, and years of education as covariates in all linear regression models. We used non-parametric bootstrap with 5000 Monte Carlo draws to estimate bias-corrected and accelerated confidence intervals for ACME and ADE.

Longitudinal analyses

All visits included in longitudinal analyses were within ± 5 years of baseline FTP PET and participants were non-demented at each visit. In the BLSA, there were a total of 167 FTP PET, 277 PiB PET, and 366 MRI scans. For BLSA participants with at least two scans, the median (interquartile range) time interval in years between last and first scan included in the longitudinal analyses was 2 (1.6, 2.2) for FTP PET, 3.9 (2.4, 4.8) for PiB PET, and 4.3 (4, 5.6) for MRI. In the ADNI, there were a total of 211 FTP PET, 194 FDG PET, and 229 MRI scans. For ADNI participants with at least two scans, the median (interquartile range) time interval in years between last and first scan included in the longitudinal analyses was 1.7 (1.1, 2.1) for FTP PET, 4.4 (4, 5) for FDG PET, and 1.3 (1.1, 2.1) for MRI.

We investigated whether amyloid is associated with the longitudinal rate of tau accumulation in the EC and ITG using separate linear mixed effects models. Outcome variables were EC and ITG tau. We included baseline age, time from baseline, sex, years of education, *APOE* $\varepsilon 4$ positivity, amyloid status, and amyloid $\times$ time interaction as fixed effects. The model for ITG tau additionally included EC tau and its two-way interactions with amyloid and time as fixed effects. For the analyses investigating the association of amyloid and ITG tau with the longitudinal change in proxies of ITG neurodegeneration, outcome variables were ITG CBF, glucose metabolism, and volume. We included baseline age, time from baseline, sex, years of education, *APOE* $\varepsilon 4$ positivity, amyloid status, ITG tau, amyloid $\times$ ITG tau, amyloid $\times$ time, and ITG tau $\times$ time interactions as fixed effects.

All linear mixed effects models included a random intercept per participant. Random slopes were included only if the total number of observations was greater than the number of random effects to ensure parameter identifiability. The only model that met this criterion and included a random slope per participant was the model for ITG volume in the BLSA.

Software

We used https://causalfusion.net/ (***Bareinboim and Pearl, 2016***) to verify the logical expressions for the conditional independencies implied by our DAGs. All statistical analyses were conducted in R

(https://cran.r-project.org, version 4.0.3). We used the `bnlearn` (***Scutari, 2010***) package to test for conditional independence, `lmerTest` (***Kuznetsova et al., 2017***) to fit the linear mixed effects models, `performance` (***Lüdecke et al., 2020***) to check model diagnostics, `mediation` (***Tingley et al., 2014***) to perform the mediation analyses, `tidyverse` (***Wickham et al., 2019***) for data wrangling and plotting, `ggExtra` (***Attali and Baker, 2019***), `ggthemes` (***Arnold, 2021***), and `wesanderson` (***Ram and Wickham, 2018***) to generate plots, `ggpubr` (***Kassambara, 2018***) to create panel figures, `stargazer` (***Hlavac, 2018***) to tabulate model results, and `knitr` (***Xie, 2018***) to generate the manuscript directly incorporating results from R.

Code and data availability

Code for performing statistical analyses and generating figures is provided in an open repository (https://gitlab.com/bilgelm/tau_amyloid_neurodegeneration). Data from the BLSA are available upon request from the BLSA website (https://www.blsa.nih.gov). All requests are reviewed by the BLSA Data Sharing Proposal Review Committee. A deidentified version (with age bands instead of continuous age and excluding APOE genotype) of the cross-sectional BLSA data used in the statistical analyses is publicly available (https://doi.org/10.7910/DVN/YFJAZO). Data from the ADNI are available from the ADNI website (adni.loni.usc.edu).

Acknowledgments

We thank Dr. Andrea Shafer and Dr. Fırat Bilgel for their thoughtful feedback.

This study was supported by the Intramural Research Program of the National Institute on Aging, NIH.

Data collection and sharing for the ADNI sample was funded by the Alzheimer's Disease Neuroimaging Initiative (ADNI) (National Institutes of Health Grant U01 AG024904) and DOD ADNI (Department of Defense award number W81XWH-12-2-0012). ADNI is funded by the National Institute on Aging, the National Institute of Biomedical Imaging and Bioengineering, and through generous contributions from the following: AbbVie, Alzheimer's Association; Alzheimer's Drug Discovery Foundation; Araclon Biotech; BioClinica, Inc.; Biogen; Bristol-Myers Squibb Company; CereSpir, Inc.; Cogstate; Eisai Inc.; Elan Pharmaceuticals, Inc.; Eli Lilly and Company; EuroImmun; F. Hoffmann-La Roche Ltd and its affiliated company Genentech, Inc.; Fujirebio; GE Healthcare; IXICO Ltd.; Janssen Alzheimer Immunotherapy Research & Development, LLC.; Johnson & Johnson Pharmaceutical Research & Development LLC.; Lumosity; Lundbeck; Merck & Co., Inc.; Meso Scale Diagnostics, LLC.; NeuroRx Research; Neurotrack Technologies; Novartis Pharmaceuticals Corporation; Pfizer Inc.; Piramal Imaging; Servier; Takeda Pharmaceutical Company; and Transition Therapeutics. The Canadian Institutes of Health Research is providing funds to support ADNI clinical sites in Canada. Private sector contributions are facilitated by the Foundation for the National Institutes of Health (www.fnih.org). The grantee organization is the Northern California Institute for Research and Education, and the study is coordinated by the Alzheimer's Therapeutic Research Institute at the University of Southern California. ADNI data are disseminated by the Laboratory for Neuro Imaging at the University of Southern California.

Competing interests

MB, LF, ARM, and SMR declare that they have no competing interests. DFW is a former President of the Brain Imaging Council of the Society of Nuclear Medicine and Molecular Imaging. DFW receives contract funding from LB Pharmaceuticals and in-kind contributions from Roche Neuroscience, Avid Radiopharmaceuticals/Eli Lilly and Company, and Cerveau Technologies.

References

Albrecht D, Lisette Isenberg A, Stradford J, Monreal T, Sagare A, Pachicano M, Sweeney M, Toga A, Zlokovic B, Chui H, Joe E, Schneider L, Conti P, Jann K, Pa J. Associations between vascular function and Tau PET

are associated with global cognition and amyloid. Journal of Neuroscience. 2020; 40(44):8573–8586. doi: 10.1523/JNEUROSCI.1230-20.2020.

Arnold JB, ggthemes: Extra Themes, Scales and Geoms for 'ggplot2'; 2021.

Attali D, Baker C, ggExtra: Add Marginal Histograms to 'ggplot2', and More 'ggplot2' Enhancements; 2019. https://cran.r-project.org/package=ggExtra.

Bareinboim E, Pearl J. Causal inference and the data-fusion problem. Proceedings of the National Academy of Sciences of the United States of America. 2016; 113(27):7345–7352. doi: 10.1073/pnas.1510507113.

Berron D, Vogel JW, Insel PS, Pereira JB, Xie L, Wisse LEM, Yushkevich PA, Palmqvist S, Mattsson-Carlgren N, Stomrud E, Smith R, Strandberg O, Hansson O. Early stages of tau pathology and its associations with functional connectivity, atrophy and memory. Brain. 2021; (2021). http://www.ncbi.nlm.nih.gov/pubmed/33725124, doi: 10.1093/brain/awab114.

Bilgel M, Beason-Held L, An Y, Zhou Y, Wong DF, Resnick SM. Longitudinal evaluation of surrogates of regional cerebral blood flow computed from dynamic amyloid PET imaging. Journal of Cerebral Blood Flow & Metabolism. 2019; doi: 10.1177/0271678X19830537.

Bischof GN, Jessen F, Fliessbach K, Dronse J, Hammes J, Neumaier B, Onur O, Fink GR, Kukolja J, Drzezga A, van Eimeren T. Impact of tau and amyloid burden on glucose metabolism in Alzheimer's disease. Annals of Clinical and Translational Neurology. 2016; 3(12):934–939. doi: 10.1002/acn3.339.

Buckley RF, Mormino EC, Chhatwal J, Schultz AP, Rabin JS, Rentz DM, Acar D, Properzi MJ, Dumurgier J, Jacobs H, Gomez-Isla T, Johnson KA, Sperling RA, Hanseeuw BJ. Associations between baseline amyloid, sex, and APOE on subsequent tau accumulation in cerebrospinal fluid. Neurobiology of Aging. 2019; 78:178–185. doi: 10.1016/j.neurobiolaging.2019.02.019.

Calafate S, Buist A, Miskiewicz K, Vijayan V, Daneels G, de Strooper B, de Wit J, Verstreken P, Moechars D. Synaptic Contacts Enhance Cell-to-Cell Tau Pathology Propagation. Cell Reports. 2015; 11(8):1176–1183. http://dx.doi.org/10.1016/j.celrep.2015.04.043, doi: 10.1016/j.celrep.2015.04.043.

Carbonell F, Zijdenbos AP, Bedell BJ. Spatially Distributed Amyloid-β Reduces Glucose Metabolism in Mild Cognitive Impairment. Journal of Alzheimer's Disease. 2020; 73(2):543–557. doi: 10.3233/JAD-190560.

Chételat G, Villemagne VL, Bourgeat P, Pike KE, Jones G, Ames D, Ellis Ka, Szoeke C, Martins RN, O'Keefe GJ, Salvado O, Masters CL, Rowe CC, Australian Imaging Biomarkers and Lifestyle Research Group. Relationship between atrophy and β-amyloid deposition in Alzheimer disease. Annals of Neurology. 2010 mar; 67(3):317–324. http://www.ncbi.nlm.nih.gov/pubmed/20373343, doi: 10.1002/ana.21955.

De Calignon A, Polydoro M, Suárez-Calvet M, William C, Adamowicz DH, Kopeikina KJ, Pitstick R, Sahara N, Ashe KH, Carlson GA, Spires-Jones TL, Hyman BT. Propagation of Tau Pathology in a Model of Early Alzheimer's Disease. Neuron. 2012; 73(4):685–697. doi: 10.1016/j.neuron.2011.11.033.

Desikan RS, Ségonne F, Fischl B, Quinn BT, Dickerson BC, Blacker D, Buckner RL, Dale AM, Maguire RP, Hyman BT, Albert MS, Killiany RJ. An automated labeling system for subdividing the human cerebral cortex on MRI scans into gyral based regions of interest. NeuroImage. 2006 jul; 31(3):968–980. http://www.ncbi.nlm.nih.gov/pubmed/16530430, doi: 10.1016/j.neuroimage.2006.01.021.

Doshi J, Erus G, Habes M, Davatzikos C. DeepMRSeg: A convolutional deep neural network for anatomy and abnormality segmentation on MR images. arXiv. 2019 jul; http://arxiv.org/abs/1907.02110.

Doshi J, Erus G, Ou Y, Resnick SM, Gur RC, Gur RE, Satterthwaite TD, Furth S, Davatzikos C. MUSE: MUlti-atlas region Segmentation utilizing Ensembles of registration algorithms and parameters, and locally optimal atlas selection. NeuroImage. 2016 feb; 127(2016):186–195. http://dx.doi.org/10.1016/j.neuroimage.2015.11.073https://linkinghub.elsevier.com/retrieve/pii/S1053811915011106, doi: 10.1016/j.neuroimage.2015.11.073.

Esparza TJ, Zhao H, Cirrito JR, Cairns NJ, Bateman RJ, Holtzman DM, Brody DL. Amyloid-beta oligomerization in Alzheimer dementia versus high-pathology controls. Annals of Neurology. 2013; 73(1):104–119. doi: 10.1002/ana.23748.

Franzmeier N, Dewenter A, Frontzkowski L, Dichgans M, Rubinski A, Neitzel J, Smith R, Strandberg O, Ossenkoppele R, Buerger K, Duering M, Hansson O, Ewers M. Patient-centered connectivity-based prediction of tau pathology spread in Alzheimer's disease. Science Advances. 2020; 6(48). doi: 10.1126/sciadv.abd1327.

Franzmeier N, Neitzel J, Rubinski A, Smith R, Strandberg O, Ossenkoppele R, Hansson O, Ewers M. Functional brain architecture is associated with the rate of tau accumulation in Alzheimer's disease. Nature communications. 2020; 11(1):347. doi: 10.1038/s41467-019-14159-1.

Fuld PA. Psychological testing in the differential diagnosis of the dementias. In: Katzman R, Terry RD, Bick KL, editors. *Alzheimer's disease: Senile dementia and related disorders* New York, NY: Raven Press; 1978.p. 185–193.

Gómez-Isla T, Hollister R, West H, Mui S, Growdon JH, Petersen RC, Parisi JE, Hyman BT. Neuronal loss correlates with but exceeds neurofibrillary tangles in Alzheimer's disease. Annals of Neurology. 1997; 41(1):17–24. doi: 10.1002/ana.410410106.

Gordon BA, McCullough A, Mishra S, Blazey TM, Su Y, Christensen J, Dincer A, Jackson K, Hornbeck RC, Morris JC, Ances BM, Benzinger TLS. Cross-sectional and longitudinal atrophy is preferentially associated with tau rather than amyloid β positron emission tomography pathology. Alzheimer's and Dementia: Diagnosis, Assessment and Disease Monitoring. 2018; 10:245–252. doi: 10.1016/j.dadm.2018.02.003.

Hanseeuw BJ, Betensky RA, Jacobs HIL, Schultz AP, Sepulcre J, Becker JA, Cosio DMO, Farrell M, Quiroz YT, Mormino EC, Buckley RF, Papp KV, Amariglio RA, Dewachter I, Ivanoiu A, Huijbers W, Hedden T, Marshall GA, Chhatwal JP, Rentz DM, et al. Association of Amyloid and Tau with Cognition in Preclinical Alzheimer Disease: A Longitudinal Study. JAMA Neurology. 2019; 76(8):915–924. doi: 10.1001/jamaneurol.2019.1424.

Hanseeuw BJ, Betensky RA, Schultz AP, Papp KV, Mormino EC, Sepulcre J, Bark JS, Cosio DM, LaPoint M, Chhatwal JP, Rentz DM, Sperling RA, Johnson KA. Fluorodeoxyglucose metabolism associated with tau-amyloid interaction predicts memory decline. Annals of Neurology. 2017; 81(4):583–596. doi: 10.1002/ana.24910.

Harrison TM, La Joie R, Maass A, Baker SL, Swinnerton K, Fenton L, Mellinger TJ, Edwards L, Pham J, Miller BL, Rabinovici GD, Jagust WJ. Longitudinal tau accumulation and atrophy in aging and Alzheimer's disease. Annals of Neurology. 2018; doi: 10.1002/ana.25406.

Hlavac M, stargazer: Well-formatted regression and summary statistics tables; 2018. https://cran.r-project.org/package=stargazer.

Iaccarino L, Tammewar G, Ayakta N, Baker SL, Bejanin A, Boxer AL, Gorno-Tempini ML, Janabi M, Kramer JH, Lazaris A, Lockhart SN, Miller BL, Miller ZA, O'Neil JP, Ossenkoppele R, Rosen HJ, Schonhaut DR, Jagust WJ, Rabinovici GD. Local and distant relationships between amyloid, tau and neurodegeneration in Alzheimer's Disease. NeuroImage: Clinical. 2018; 17(September 2017):452–464. http://dx.doi.org/10.1016/j.nicl.2017.09.016, doi: 10.1016/j.nicl.2017.09.016.

Imai K, Keele L, Yamamoto T. Identification, inference and sensitivity analysis for causal mediation effects. Statistical Science. 2010; 25(1):51–71. doi: 10.1214/10-STS321.

Jack CR, Twomey K, Zinsmeister AR, Sharbrough FW, Petersen C, Cascino GD. Anterior temporal lobes and hippocampal formations: normative volumetric measurements from MR images in young adults. Radiology. 1989; 172:549–554.

Jack CR, Wiste HJ, Schwarz CG, Lowe VJ, Senjem ML, Vemuri P, Weigand SD, Therneau TM, Knopman DS, Gunter JL, Jones DT, Graff-Radford J, Kantarci K, Roberts RO, Mielke MM, Machulda MM, Petersen RC. Longitudinal tau PET in ageing and Alzheimer's disease. Brain. 2018; 141(5):1517–1528. https://academic.oup.com/brain/advance-article/doi/10.1093/brain/awy059/4929907, doi: 10.1093/brain/awy059.

Jack CR, Wiste HJ, Weigand SD, Therneau TM, Knopman DS, Lowe V, Vemuri P, Mielke MM, Roberts RO, Machulda MM, Senjem ML, Gunter JL, Rocca WA, Petersen RC. Age-specific and sex-specific prevalence of cerebral β-amyloidosis, tauopathy, and neurodegeneration in cognitively unimpaired individuals aged 50–95 years: a cross-sectional study. The Lancet Neurology. 2017; 4422(17). http://linkinghub.elsevier.com/retrieve/pii/S1474442217300777, doi: 10.1016/S1474-4422(17)30077-7.

Jack CR, Wiste HJ, Weigand SD, Therneau TM, Lowe VJ, Knopman DS, Botha H, Graff-Radford J, Jones DT, Ferman TJ, Boeve BF, Kantarci K, Vemuri P, Mielke MM, Whitwell J, Josephs K, Schwarz CG, Senjem ML, Gunter JL, Petersen RC. Predicting future rates of tau accumulation on PET. Brain. 2020 oct; 143(10):3136–3150. https://academic.oup.com/brain/advance-article/doi/10.1093/brain/awaa248/5930009https://academic.oup.com/brain/article/143/10/3136/5930009, doi: 10.1093/brain/awaa248.

Jacobs HIL, Hedden T, Schultz AP, Sepulcre J, Perea RD, Amariglio RE, Papp KV, Rentz DM, Sperling RA, Johnson KA. Structural tract alterations predict downstream tau accumulation in amyloid-positive older individuals. Nature Neuroscience. 2018; 21(3):424–431. http://dx.doi.org/10.1038/s41593-018-0070-z, doi: 10.1038/s41593-018-0070-z.

Jansen WJ, Ossenkoppele R, Knol DL, Tijms BM, Scheltens P, Verhey FRJ, Visser PJ, Aalten P, Aarsland D, Alcolea D, Alexander M, Almdahl IS, Arnold SE, Baldeiras I, Barthel H, van Berckel BNM, Bibeau K, Blennow K, Brooks DJ, van Buchem Ma, et al. Prevalence of cerebral amyloid pathology in persons without dementia. JAMA. 2015; 313(19):1924–1938. http://jama.jamanetwork.com/article.aspx?doi=10.1001/jama.2015.4668, doi: 10.1001/jama.2015.4668.

Jin M, Shepardson N, Yang T, Chen G, Walsh D, Selkoe DJ. Soluble amyloid β-protein dimers isolated from Alzheimer cortex directly induce Tau hyperphosphorylation and neuritic degeneration. Proceedings of the National Academy of Sciences of the United States of America. 2011; 108(14):5819–5824. doi: 10.1073/pnas.1017033108.

Kassambara A, ggpubr: 'ggplot2' based publication ready plots; 2018. https://cran.r-project.org/package=ggpubr.

Korte N, Nortley R, Attwell D. Cerebral blood flow decrease as an early pathological mechanism in Alzheimer's disease. Acta Neuropathologica. 2020; 140(6):793–810. https://doi.org/10.1007/s00401-020-02215-w, doi: 10.1007/s00401-020-02215-w.

Kuznetsova A, Brockhoff PB, Christensen RHB. lmerTest Package: Tests in Linear Mixed Effects Models . Journal of Statistical Software. 2017; 82(13). doi: 10.18637/jss.v082.i13.

La Joie R, Visani AV, Baker SL, Brown JA, Bourakova V, Cha J, Chaudhary K, Edwards L, Iaccarino L, Janabi M, Lesman-Segev OH, Miller ZA, Perry DC, O'Neil JP, Pham J, Rojas JC, Rosen HJ, Seeley WW, Tsai RM, Miller BL, et al. Prospective longitudinal atrophy in Alzheimer's disease correlates with the intensity and topography of baseline tau-PET. Science Translational Medicine. 2020 jan; 12(524):eaau5732. http://stm.sciencemag.org/lookup/doi/10.1126/scitranslmed.aau5732, doi: 10.1126/scitranslmed.aau5732.

Landau SM, Harvey D, Madison CM, Koeppe RA, Reiman EM, Foster NL, Weiner MW, Jagust WJ. Associations between cognitive, functional, and FDG-PET measures of decline in AD and MCI. Neurobiology of Aging. 2011 jul; 32(7):1207–1218. http://www.pubmedcentral.nih.gov/articlerender.fcgi?artid=2891865{&}tool=pmcentrez{&}rendertype=abstract, doi: 10.1016/j.neurobiolaging.2009.07.002.

Liu L, Drouet V, Wu JW, Witter MP, Small SA, Clelland C, Duff K. Trans-synaptic spread of tau pathology in vivo. PLoS ONE. 2012; 7(2):1–9. doi: 10.1371/journal.pone.0031302.

Lüdecke D, Makowski D, Waggoner P, Patil I, performance: Assessment of Regression Models Performance; 2020. https://easystats.github.io/performance/, doi: 10.5281/zenodo.3952174.

Mak E, Bethlehem RAI, Romero-Garcia R, Cervenka S, Rittman T, Gabel S, Surendranathan A, Bevan-Jones RW, Passamonti L, Vázquez Rodríguez P, Su L, Arnold R, Williams GB, Hong YT, Fryer TD, Aigbirhio FI, Rowe JB, O'Brien JT. In vivo coupling of tau pathology and cortical thinning in Alzheimer's disease. Alzheimer's and Dementia: Diagnosis, Assessment and Disease Monitoring. 2018; 10:678–687. doi: 10.1016/j.dadm.2018.08.005.

McKee AC, Kosik KS, Kowall NW. Neuritic pathology and dementia in alzheimer's disease. Annals of Neurology. 1991; 30(2):156–165. doi: 10.1002/ana.410300206.

Mintun MA, Lo AC, Duggan Evans C, Wessels AM, Ardayfio PA, Andersen SW, Shcherbinin S, Sparks J, Sims JR, Brys M, Apostolova LG, Salloway SP, Skovronsky DM. Donanemab in Early Alzheimer's Disease. New England Journal of Medicine. 2021 may; 384(18):1691–1704. http://www.nejm.org/doi/10.1056/NEJMoa2100708, doi: 10.1056/NEJMoa2100708.

Morris JC. The Clinical Dementia Rating (CDR): Current version and scoring rules. Neurology. 1993; 43(11):2412–2414.

Morsch R, Simon W, Coleman PD. Neurons may live for decades with neurofibrillary tangles. Journal of Neuropathology & Experimental Neurology. 1999; 58(2):188–197.

Nelson PT, Alafuzoff I, Bigio EH, Bouras C, Braak H, Cairns NJ, Castellani RJ, Crain BJ, Davies P, Del Tredici K, Duyckaerts C, Frosch MP, Haroutunian V, Hof PR, Hulette CM, Hyman BT, Iwatsubo T, Jellinger KA, Jicha GA, Kövari E, et al. Correlation of Alzheimer disease neuropathologic changes with cognitive status: a review of the literature. Journal of Neuropathology and Experimental Neurology. 2012 may; 71(5):362–381. https://academic.oup.com/jnen/article-lookup/doi/10.1097/NEN.0b013e31825018f7http://www.ncbi.nlm.nih.gov/pubmed/22487856http://www.pubmedcentral.nih.gov/articlerender.fcgi?artid=PMC3560290, doi: 10.1097/NEN.0b013e31825018f7.

Novak P, Kovacech B, Katina S, Schmidt R, Scheltens P, Kontsekova E, Ropele S, Fialova L, Kramberger M, Paulenka-Ivanovova N, Smisek M, Hanes J, Stevens E, Kovac A, Sutovsky S, Parrak V, Koson P, Prcina M, Galba J, Cente M, et al. ADAMANT: a placebo-controlled randomized phase 2 study of AADvac1, an active immunotherapy against pathological tau in Alzheimer's disease. Nature Aging. 2021; 1(6):521–534. https://doi.org/10.1038/s43587-021-00070-2, doi: 10.1038/s43587-021-00070-2.

Pearl J. Interpretation and identification of causal mediation. Psychological Methods. 2014; 19(4):459–481. http://doi.apa.org/getdoi.cfm?doi=10.1037/a0036434, doi: 10.1037/a0036434.

Petersen RC. Mild cognitive impairment as a diagnostic entity. Journal of Internal Medicine. 2004; 256(3):183–194. doi: 10.1111/j.1365-2796.2004.01388.x.

Petersen RC, Aisen PS, Beckett LA, Donohue MC, Gamst AC, Harvey DJ, Jack CR, Jagust WJ, Shaw LM, Toga AW. Alzheimer's Disease Neuroimaging Initiative (ADNI) clinical characterization. Neurology. 2010; 74(3):201–209.

Petersen RC, Wiste HJ, Weigand SD, Rocca WA, Roberts RO, Mielke MM, Lowe VJ, Knopman DS, Pankratz VS, Machulda MM, Geda YE, Jack Jr CR. Association of elevated amyloid levels with cognition and biomarkers in cognitively normal people from the community. JAMA Neurology. 2016; 73(1):85–92. doi: 10.1001/jamaneurol.2015.3098.

Pooler AM, Polydoro M, Maury EA, Nicholls SB, Reddy SM, Wegmann S, William C, Saqran L, Cagsal-Getkin O, Pitstick R, Beier DR, Carlson GA, Spires-Jones TL, Hyman BT. Amyloid accelerates tau propagation and toxicity in a model of early Alzheimer's disease. Acta Neuropathologica Communications. 2015 dec; 3(1):14. http://actaneurocomms.biomedcentral.com/articles/10.1186/s40478-015-0199-x, doi: 10.1186/s40478-015-0199-x.

Ram K, Wickham H, wesanderson: A Wes Anderson Palette Generator; 2018.

Rousset OG, Ma Y, Evans AC. Correction for partial volume effects in PET: principle and validation. Journal of Nuclear Medicine. 1998; 39(5):904–911.

Rubinski A, Tosun D, Franzmeier N, Neitzel J, Frontzkowski L, Weiner M, Ewers M. Lower cerebral perfusion is associated with tau-PET in the entorhinal cortex across the Alzheimer's continuum. Neurobiology of Aging. 2021; 102:111–118. https://doi.org/10.1016/j.neurobiolaging.2021.02.003, doi: 10.1016/j.neurobiolaging.2021.02.003.

Salvadó G, Grothe MJ, Groot C, Moscoso A, Schöll M, Gispert JD, Ossenkoppele R. Differential associations of APOE-ϵ2 and APOE-ϵ4 alleles with PET-measured amyloid-β and tau deposition in older individuals without dementia. European Journal of Nuclear Medicine and Molecular Imaging. 2021 feb; 16. http://link.springer.com/10.1007/s00259-021-05192-8, doi: 10.1007/s00259-021-05192-8.

Sanchez JS, Becker JA, Jacobs HIL, Hanseeuw BJ, Jiang S, Schultz AP, Properzi MJ, Katz SR, Beiser A, Satizabal CL, O'Donnell A, DeCarli C, Killiany R, El Fakhri G, Normandin MD, Gómez-Isla T, Quiroz YT, Rentz DM, Sperling RA, Seshadri S, et al. The cortical origin and initial spread of medial temporal tauopathy in Alzheimer's disease assessed with positron emission tomography. Science Translational Medicine. 2021 jan; 13(577):eabc0655. https://stm.sciencemag.org/lookup/doi/10.1126/scitranslmed.abc0655, doi: 10.1126/scitranslmed.abc0655.

Schreiber S, Landau SM, Fero A, Schreiber F, Jagust WJ. Comparison of visual and quantitative florbetapir F 18 positron emission tomography analysis in predicting mild cognitive impairment outcomes. JAMA Neurology. 2015; 72(10):1183–1190. doi: 10.1001/jamaneurol.2015.1633.

Scott MR, Hampton OL, Buckley RF, Chhatwal JP, Hanseeuw BJ, Jacobs HI, Properzi MJ, Sanchez JS, Johnson KA, Sperling RA, Schultz AP. Inferior temporal tau is associated with accelerated prospective cortical thinning in clinically normal older adults. NeuroImage. 2020; 220(March):116991. https://doi.org/10.1016/j.neuroimage.2020.116991, doi: 10.1016/j.neuroimage.2020.116991.

Scutari M. Learning Bayesian Networks wirth bnlearn R package. Journal of Statistical Software. 2010; 35(3).

Sokoloff L. Sites and mechanisms of function-related changes in energy metabolism in the nervous system. Developmental Neuroscience. 1993; 15(3-5):194–206. doi: 10.1159/000111335.

Sperling RA, Aisen PS, Beckett LA, Bennett DA, Craft S, Fagan AM, Iwatsubo T, Jack CR, Kaye J, Montine TJ, Park DC, Reiman EM, Rowe CC, Siemers E, Stern Y, Yaffe K, Carrillo MC, Thies B, Morrison-Bogorad M, Wagster MV, et al. Toward defining the preclinical stages of Alzheimer's disease: recommendations from the National Institute on Aging-Alzheimer's Association workgroups on diagnostic guidelines for Alzheimer's disease. Alzheimer's & Dementia. 2011 may; 7(3):280–292. http://www.pubmedcentral.nih.gov/articlerender.fcgi?artid=3220946{&}tool=pmcentrez{&}rendertype=abstract, doi: 10.1016/j.jalz.2011.03.003.

Strom A, Iaccarino L, Edwards L, Lesman-Segev OH, Soleimani-Meigooni DN, Pham J, Baker SL, Landau S, Jagust WJ, Miller BL, Rosen HJ, Gorno-Tempini ML, Rabinovici GD, La Joie R. Cortical hypometabolism reflects local atrophy and tau pathology in symptomatic Alzheimer's disease. Brain. 2021 aug; doi: 10.1093/brain/awab294.

Teipel S, Grothe MJ. Does posterior cingulate hypometabolism result from disconnection or local pathology across preclinical and clinical stages of Alzheimer's disease? European Journal of Nuclear Medicine and Molecular Imaging. 2016; 43(3):526–536. doi: 10.1007/s00259-015-3222-3.

Thomas BA, Erlandsson K, Modat M, Thurfjell L, Vandenberghe R, Ourselin S, Hutton BF. The importance of appropriate partial volume correction for PET quantification in Alzheimer's disease. European Journal of Nuclear Medicine and Molecular Imaging. 2011 jun; 38(6):1104–1119. http://www.ncbi.nlm.nih.gov/pubmed/21336694http://link.springer.com/10.1007/s00259-011-1745-9, doi: 10.1007/s00259-011-1745-9.

Tingley D, Yamamoto T, Hirose K, Keele L, Imai K. mediation: R Package for Causal Mediation Analysis. Journal of Statistical Software. 2014; 59(5).

Villemagne VL, Burnham S, Bourgeat P, Brown B, Ellis KA, Salvado O, Szoeke C, Macaulay SL, Martins R, Maruff P, Ames D, Rowe CC, Masters CL. Amyloid β deposition, neurodegeneration, and cognitive decline in sporadic Alzheimer's disease: a prospective cohort study. Lancet Neurology. 2013 apr; 12(4):357–367. http://www.ncbi.nlm.nih.gov/pubmed/23477989, doi: 10.1016/S1474-4422(13)70044-9.

Wickham H, Averick M, Bryan J, Chang W, McGowan L, François R, Grolemund G, Hayes A, Henry L, Hester J, Kuhn M, Pedersen T, Miller E, Bache S, Müller K, Ooms J, Robinson D, Seidel D, Spinu V, Takahashi K, et al. Welcome to the Tidyverse. Journal of Open Source Software. 2019; 4(43):1686. doi: 10.21105/joss.01686.

Wu J, Hussaini S, Bastille I. Neuronal activity enhances tau propagation and tau pathology in vivo. Nat Neurosci. 2016; 19(8):1085–1092. http://www.nature.com/authors/editorial{_}policies/license.html{#}terms, doi: 10.1038/nn.4328.

Xie Y, knitr: A general-purpose package for dynamic report generation in R; 2018.

Zhou Y, Resnick SM, Ye W, Fan H, Holt DP, Klunk WE, Mathis CA, Dannals R, Wong DF. Using a reference tissue model with spatial constraint to quantify [11C]Pittsburgh compound B PET for early diagnosis of Alzheimer's disease. NeuroImage. 2007 jun; 36(2):298–312. http://www.pubmedcentral.nih.gov/articlerender.fcgi?artid=2001263{&}tool=pmcentrez{&}rendertype=abstracthttps://linkinghub.elsevier.com/retrieve/pii/S1053811907001814, doi: 10.1016/j.neuroimage.2007.03.004.

Ziontz J, Bilgel M, Shafer AT, Moghekar A, Elkins W, Helphrey J, Gomez G, June D, McDonald MA, Dannals RF, Azad BB, Ferrucci L, Wong DF, Resnick SM. Tau pathology in cognitively normal older adults. Alzheimer's & Dementia: Diagnosis, Assessment & Disease Monitoring. 2019; 11:637–645. https://doi.org/10.1016/j.dadm.2019.07.007, doi: 10.1016/j.dadm.2019.07.007.

Table 1. Participant characteristics. Continuous values are reported as median (interquartile range) and categorical values are reported as N (%). Age, diagnosis, PET measures, and MRI volumes are reported at the visit corresponding to or closest to the baseline FTP PET. A– = Amyloid negative, A+ = Amyloid positive, ADNI = Alzheimer's Disease Neuroimaging Initiative, *APOE* = Apolipoprotein E, BLSA = Baltimore Longitudinal Study of Aging, FDG = fluorodeoxyglucose, FTP = flortaucipir, ICV-adj. = intracranial volume-adjusted, ITG = inferior temporal gyrus, MRI = magnetic resonance imaging, PiB = Pittsburgh compound B, R_1 = relative radiotracer delivery parameter, SUVR = standardized update value ratio.

	BLSA		ADNI	
	A–, N = 71	**A+**, N = 32	**A–**, N = 61	**A+**, N = 61
Age at baseline FTP PET (years)	77 (70, 83)	78 (73, 87)	76 (70, 81)	75 (71, 80)
Sex				
Female	43 (61%)	16 (50%)	21 (34%)	33 (54%)
Male	28 (39%)	16 (50%)	40 (66%)	28 (46%)
Race				
Asian or Pacific Islander	4 (6%)	1 (3%)	1 (2%)	–
Black	13 (18%)	4 (12%)	2 (3%)	4 (7%)
White	54 (76%)	27 (84%)	57 (93%)	56 (92%)
Other	–	–	1 (2%)	1 (2%)
APOE status				
$\varepsilon 4-$	51 (72%)	20 (62%)	52 (85%)	27 (44%)
$\varepsilon 4+$	20 (28%)	12 (38%)	9 (15%)	34 (56%)
Education (years)	18 (16, 20)	17 (16, 18)	18 (16, 19)	16 (14, 18)
Diagnosis at baseline FTP PET				
Cognitively normal	70 (99%)	25 (78%)	11 (18%)	11 (18%)
Mild cognitive impairment	1 (1%)	7 (22%)	50 (82%)	50 (82%)
PET measures at baseline FTP PET				
Entorhinal cortex FTP SUVR	1.02 (0.93, 1.1)	1.07 (1.01, 1.23)	1.91 (1.74, 2.34)	2.44 (2.02, 2.97)
ITG FTP SUVR	1.24 (1.19, 1.32)	1.37 (1.29, 1.49)	1.92 (1.8, 2.02)	2.05 (1.91, 2.62)
ITG PiB R_1	0.88 (0.86, 0.9)	0.85 (0.82, 0.9)	–	–
ITG FDG SUVR	–	–	1.22 (1.17, 1.31)	1.21 (1.12, 1.32)
ITG volume (ICV-adj. residual, cm^3)	-0.51 (-1.45, 0.45)	-1.38 (-2.54, 0)	-0.26 (-1.67, 1.1)	-1.61 (-3.12, 0.41)
No. FTP PET per participant				
1	41 (58%)	18 (56%)	34 (56%)	26 (43%)
2	21 (30%)	9 (28%)	18 (30%)	22 (36%)
3+	9 (13%)	5 (16%)	9 (15%)	13 (21%)
No. PiB PET per participant				
1	16 (23%)	8 (25%)	–	–
2	21 (30%)	7 (22%)	–	–
3	18 (25%)	8 (25%)	–	–
4+	16 (23%)	9 (28%)	–	–
No. FDG PET per participant				
1	–	–	23 (38%)	37 (61%)
2	–	–	32 (52%)	20 (33%)
3	–	–	6 (10%)	4 (7%)
No. MRI per participant				
1	3 (4%)	1 (3%)	15 (25%)	27 (44%)
2	12 (17%)	8 (25%)	29 (48%)	25 (41%)
3	26 (37%)	11 (34%)	16 (26%)	9 (15%)
4+	30 (42%)	12 (38%)	1 (2%)	–

Appendix 1

Conditional independencies for more parsimonious DAGs

Hypothesized model

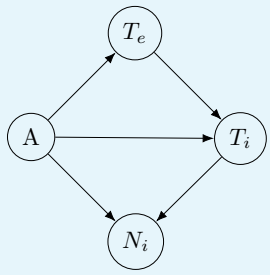

✓ $T_e \perp\!\!\!\perp N_i \mid A, T_i, G$

"A, T, N are mutually independent"

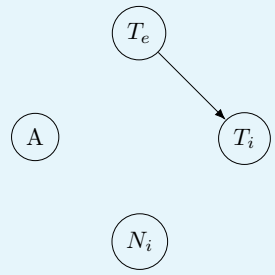

✗ $A \perp\!\!\!\perp T_e \mid G$
✗ $A \perp\!\!\!\perp T_i \mid G$
✗ $A \perp\!\!\!\perp N_i \mid G$
✗ $T_e \perp\!\!\!\perp N_i \mid G$
✗ $T_i \perp\!\!\!\perp N_i \mid G$

"A is not involved in T or N"

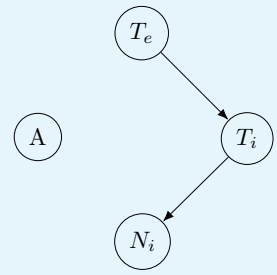

✗ $A \perp\!\!\!\perp T_e \mid G$
✗ $A \perp\!\!\!\perp T_i \mid G$
✗ $A \perp\!\!\!\perp N_i \mid G$
✓ $T_e \perp\!\!\!\perp N_i \mid T_i, G$

"A is not involved in T"

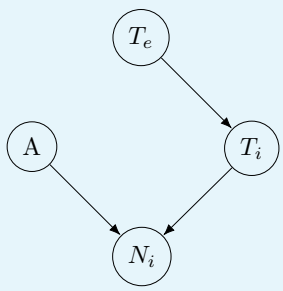

✗ $A \perp\!\!\!\perp T_e \mid G$
✗ $A \perp\!\!\!\perp T_i \mid G$
✓ $T_e \perp\!\!\!\perp N_i \mid T_i, G$

"Neither A nor T is involved in N"

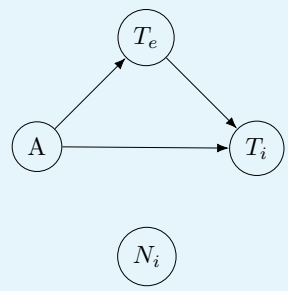

✗ $A \perp\!\!\!\perp N_i \mid G$
✗ $T_e \perp\!\!\!\perp N_i \mid G$
✗ $T_i \perp\!\!\!\perp N_i \mid G$

"A is not involved in N"

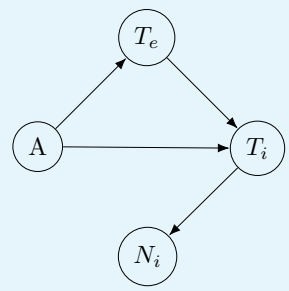

✗ $A \perp\!\!\!\perp N_i \mid T_i, G$
✓ $T_e \perp\!\!\!\perp N_i \mid T_i, G$

"A is not involved in MTL T"

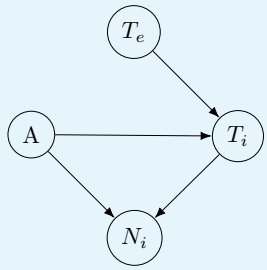

✗ $A \perp\!\!\!\perp T_e \mid G$
✓ $T_e \perp\!\!\!\perp N_i \mid A, T_i, G$

"A is not involved in neocortical T"

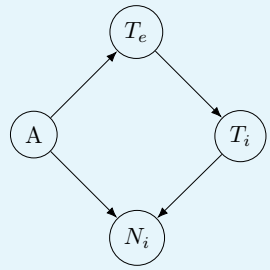

✗ $A \perp\!\!\!\perp T_i \mid T_e, G$
✓ $T_e \perp\!\!\!\perp N_i \mid A, T_i, G$

"T is not involved in N"

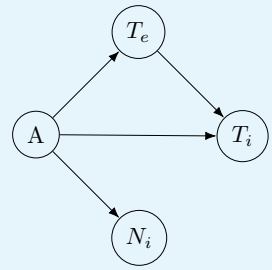

✓ $T_e \perp\!\!\!\perp N_i \mid A, G$
✗ $T_i \perp\!\!\!\perp N_i \mid A, G$

Appendix 1 Figure 1. DAGs investigated. G indicates the collection of covariates (age, sex, education, and *APOE* $\varepsilon 4$ status). Each of these covariates is a node with an arrow towards each of the four nodes shown in this diagram (nodes for covariates are not shown). The conditional independencies implied by each DAG are listed below the graphs. ✓ indicates that the partial correlation is not statistically significant in the observed data (and therefore, the DAG is not inconsistent with the data). ✗ indicates that the partial correlation is statistically significant (and therefore, the DAG is inconsistent with the data). A = binary amyloid status, T_e = EC tau, T_i = ITG tau, N_i = ITG neurodegeneration.

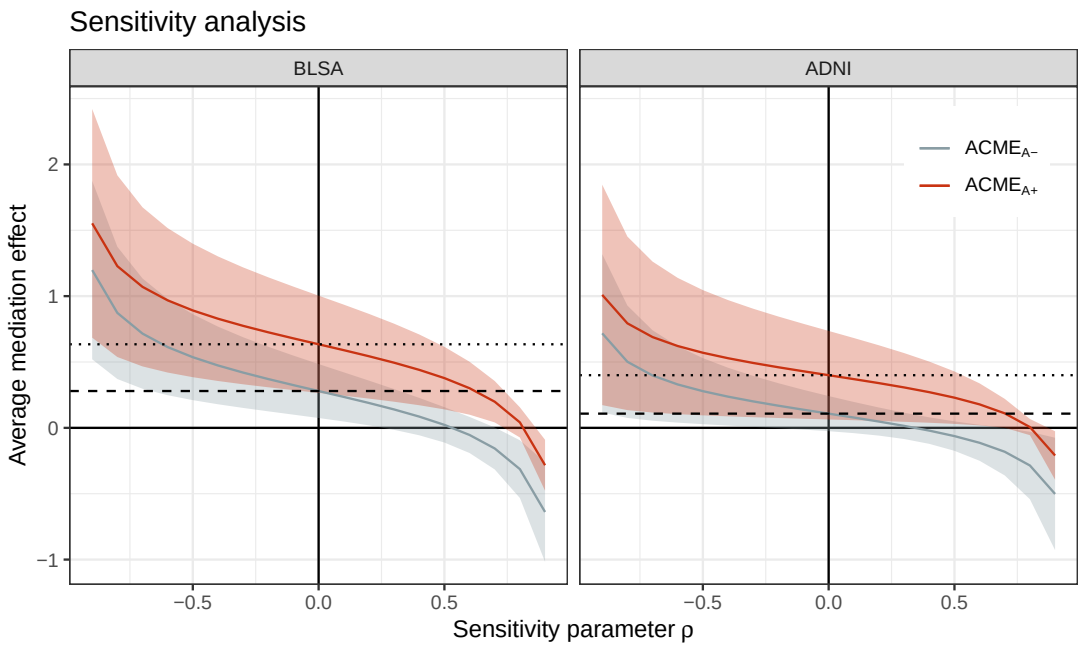

Figure 2–Figure supplement 1. Sequential ignorability assumption sensitivity analyses for the mediation models investigating entorhinal cortex tau as a mediator of the association between amyloid group and inferior temporal gyrus tau. Sensitivity parameter ρ is the simulated correlation between the mediator and the outcome model residuals. The 95% confidence interval of ACME$_{A+}$ does not include the value 0 in either data set when $\rho < 0.5$. This indicates that even in the presence of an unspecified confounder accounting for residual correlations up to 0.5 between the mediator and the outcome, our conclusion that ACME$_{A+}$ is statistically significant would hold.

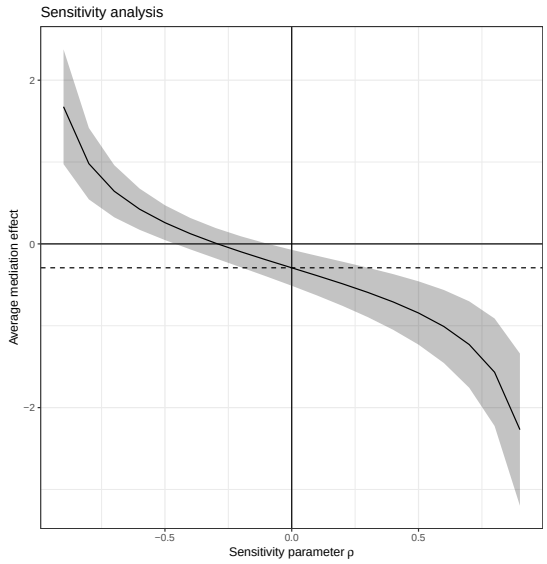

Figure 3–Figure supplement 1. Sequential ignorability assumption sensitivity analysis for the mediation model investigating inferior temporal gyrus tau as a mediator of the association between amyloid group and inferior temporal gyrus cerebral blood flow in the BLSA.

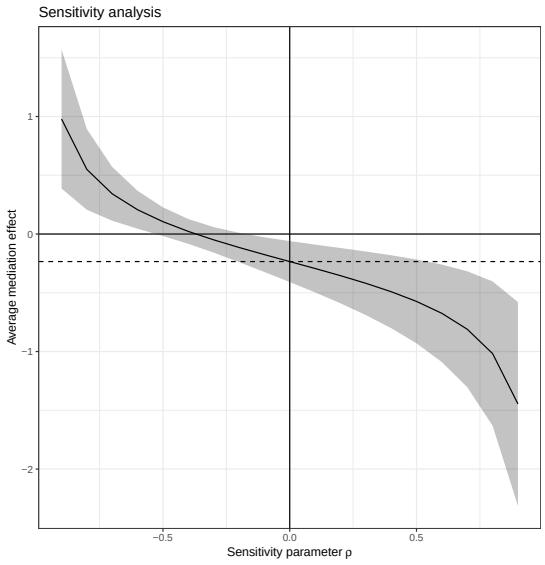

Figure 4–Figure supplement 1. Sequential ignorability assumption sensitivity analysis for the mediation model investigating inferior temporal gyrus tau as a mediator of the association between amyloid group and inferior temporal gyrus volume in the ADNI.